Spectrum-profile-identification-based wavelength division multiplexing method for a fiber Bragg grating sensor

Yuheng Pan (潘玉恒)[1,2], Junfeng Jiang (江俊峰)[1,*], Weijia Lu (鲁维佳)[2], Huijia Yang (杨会甲)[1], Kun Liu (刘 琨)[1], Shuang Wang (王 双)[1], Hui Wang (王 辉)[1], and Tiegen Liu (刘铁根)[1]

[1]*Key Laboratory of Optoelectronics Information Technology, Institute of Optical Fiber Sensing of Tianjin University, MEC, Tianjin 300072, China*

[2]*School of Computer and Information Engineering, Tianjin Chengjian University, Tianjin 300384, China*

**Corresponding author: jiangjfjxu@tju.edu.cn*

Received January 5, 2017; accepted April 7, 2017; posted online May 5, 2017

A new wavelength division multiplexing method for fiber Bragg grating (FBG) sensors based on spectrum profile identification is proposed. In this method, FBGs and tilted FBG (TFBG) sensors are cascaded in a single fiber in one sensing channel. The different spectrum profiles enable the cross-correlation method to demodulate the wavelength. Therefore, the different types of sensors can occupy the same central wavelength band. Using this method, the multiplexing capacity is optimized. Experiment results demonstrate the feasibility of this method and it is useful for applications where large numbers of FBGs are needed.

OCIS codes: 060.0060, 060.3735, 060.2370, 230.1480.
doi: 10.3788/COL201715.070605.

Fiber Bragg grating (FBG) sensors have been widely adopted in the measurement of various parameters such as temperature, strain, pressure, etc.[1]. One of the most attractive features for FBG sensors is the wavelength-encoded characteristic that makes the sensed information indifferent to light source fluctuations. The second most advantageous feature is the multiplexing capability that enables quasi-distributed sensing when dense sensing points are desired[2–4]. Wavelength division multiplexing (WDM) is the most commonly used method of FBG multiplexing techniques[5–8]. By this means, the FBG arrays are serially connected in one single fiber. The FBGs are illuminated by a broadband laser source and the reflected or transmission spectrum is acquired by a photoelectric detector (PD). The Bragg wavelengths of these FBG sensors must be different from each other so that they can be demodulated by an interrogator. In the meantime, a fixed spectral interval has to be assigned between two adjacent Bragg wavelengths according to the actual measuring range, so that no wavelength overlap would occur when the wavelengths shift in response to the changes of measurands. If there are two sensors in one fiber occupying the same wavelength window, it will introduce an error in the demodulation result. So the maximum number of multiplexed FBG sensors is restricted by the light source scanning range and by the Bragg wavelength operation ranges. To enhance the system capacity, various time division multiplexing (TDM) techniques[9–12] and the combination of WDM and TDM[13,14] are proposed. However, the TDM system lacks flexibility as it requires a fixed optical path difference (OPD) between adjacent sensor elements. Also, the cross talk and low power of reflected signals make signal processing difficult while for the combined system it required complex configurations.

In this Letter, we proposed a new multiplexing method for increasing the WDM multiplexing capacity of FBG sensors. The method cascades FBGs and tilted FBGs (TFBGs) in a single fiber. The sensors are illuminated by an amplified spontaneous emission (ASE) light source. Due to different spectrum profiles, a cross-correlation demodulation method is used to detect the wavelength shift. In this method, besides the advantages of conventional WDM systems, FBG and TFBG sensors can possess the same central wavelength, which is crucial in the occasions where numerous sensing points are desired, such as structural health monitoring applications.

The basic principle of demodulation for FBG sensors is to monitor the wavelength shift in response to the variation of the measurand. Suppose the transmission spectrum of FBG sensors have a Gaussian profile and remain constant as the central wavelength shifts. We primarily record an undisturbed spectrum $T(\lambda_i)$, $i = 1, 2, ..., N$, which is a set of digitized samples at wavelengths λ_i by a step of $\delta\lambda$ within the working scope $\lambda_{\min} - \lambda_{\max}$. The wavelength step $\delta\lambda$ is determined by the following equation:

$$\delta\lambda = \frac{\lambda_{\max} - \lambda_{\min}}{N}. \tag{1}$$

When the measurand is imposed on an FBG sensor, a perturbed spectrum $T'(\lambda_i) = T(\lambda_i - \Delta\lambda)$ is obtained, where $\Delta\lambda$ is the wavelength shift introduced by the measurand varying, which can be expressed as

$$\Delta\lambda = m\delta\lambda \qquad m = 0, 1, ..., (N-1). \tag{2}$$

The wavelength shift $\Delta\lambda$ can be calculated using cross correlation by the equation

$$R(k) = \sum_{i=0}^{N-1} T(\lambda_i)\, T(\lambda_{i+k} - \Delta\lambda), \tag{3}$$

where $R(k)$ is a vector composed of N samples. We can get the x coordinate m at which the amplitude of $R(k)$ is maximum. The wavelength shift $\Delta\lambda$ can be calculated according to Eq. (2)[15,16]. For the temperature measurement, the temperature vibration ΔT can be calculated by

$$\Delta\lambda = K_T \cdot \Delta T, \tag{4}$$

where K_T is the temperature sensitivity of FBG sensors.

The system scheme is shown in Fig. 1. The ASE source is followed by an optical fiber Fabry–Perot tunable filter (FFP-TF), which is driven by a triangular waveform, in order to scan over the whole wavelength operating range of the sensor periodically. Most of optical power (90%) enters the sensing element, which is divided into M sensing channels, and the other 10% is coupled into the Fabry–Perot (F-P) etalon, acting as a wavelength extraction element. A number of FBG or TFBG sensors are cascaded in each sensing channel. The transmission spectrum of the sensors and the F-P etalon are detected by PD arrays and then sent to a data acquisition card (DAQ) for further processing using a computer.

As the scanning wavelength range is from 1525 to 1550 nm, the sample points are set 10000 in every scanning period. We then get the 2.5 pm wavelength step according to Eq. (1). Two FBGs and a TFBG are employed in the experiment. The central wavelength of the TFBG is 1546 nm which is coincident with the FBG2, while the central wavelength of the other packaged sensor FBG1 is 1540 nm. We employ a low-temperature alcohol bath and a water bath, of which the temperature fluctuation is wihtin ± 0.01°C/30 min, to provide a steady temperature field. We placed the FBGs and TFBG sensor into the low-temperature alcohol bath with the temperature 20°C seperately and then record the respective spectra of the two FBGs and TFBG at 20°C shown in Figs. 2(a)–2(c).

The whole experiment includes two parts. First, we cascade the FBG2 and TFBG and put them into the water bath. The temperature is increased from 30°C to 90°C with a step of 10°C and the relevant spectra are expressed in Fig. 3.

Taking the separated spectra at 20°C as a reference, the cross-correlation functions between the resultant spectrum at each temperature and the reference are calculated and are shown in Fig. 4. We extracted the x coordinate of the maximum amplitude of the curves and the wavelength variation $\Delta\lambda$ can be calculated from Eq. (2).

Figure 5 shows that there is a good linear relationship between the demodulated wavelength variation and the temperature change with the linear correlation coefficients of 0.99969 and 0.99906, respectively. The measured temperature sensitivity of FBG2 is 13.6 pm/°C and that of TFBG is 11.2 pm/°C.

Second, the FBGs and TFBG are cascaded and the resultant spectrum is shown in Fig. 2(d). The temperature

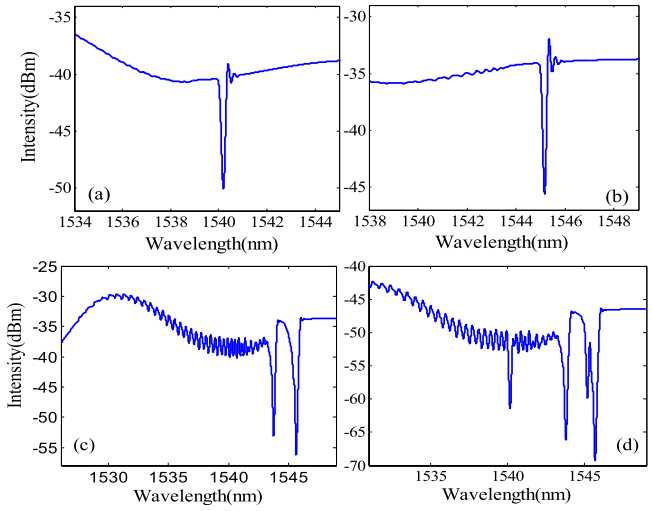

Fig. 2. Experimental spectra of the sensors at 20°C: (a) spectrum of the FBG1, (b) spectrum of the FBG2, (c) spectrum of TFBG, and (d) spectrum of cascaded FBGs and TFBG.

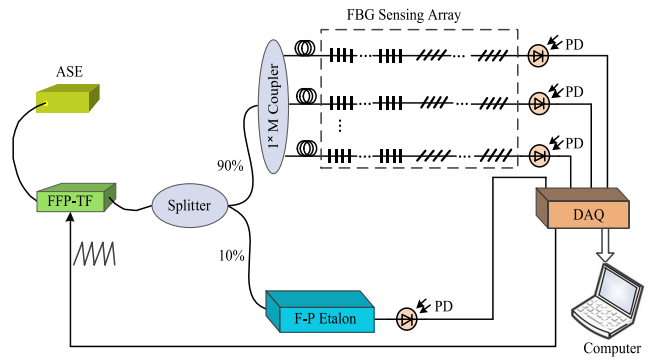

Fig. 1. Schematic diagram of the system.

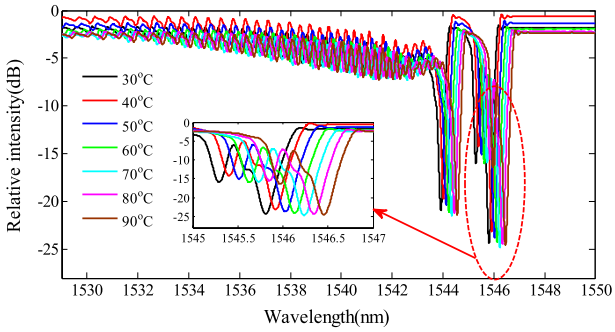

Fig. 3. (Color online) Spectra of the cascaded FBG2 and TFBG at different temperatures.

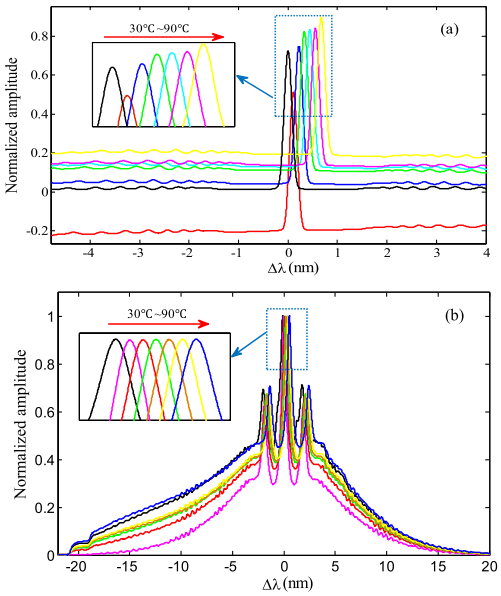

Fig. 4. (Color online) Cross-correlation curve of (a) FBG2 and (b) TFBG.

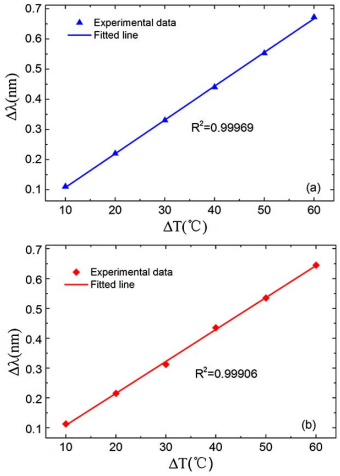

Fig. 5. Peak of the cross-correlation curve and temperature relationship of (a) FBG2 and (b) TFBG.

varies from −70°C to 20°C with a step of 10°C and the relevant spectra are expressed in Fig. 6.

The cross-correlation functions between the resultant spectrum at each temperature and the reference are calculated. Figure 7 shows the cross-correlation curves of the two FBGs and Fig. 8 is the temperature response characteristics and the linear correlation coefficients of 0.99834 and 0.98893, respectively.

The measured errors and variances are shown in Table 1. The error of the FBG2 is a little larger than that of the TFBG and FBG1, and the maximum measurement errors are within 3.23°C. Generally, in this proposed method, the maximum number of multiplexing FBGs in one chanel is two times that of the conventional WDM, which is determined by the measurement span if the scanning wavelength range of the light source is fixed. As an example,

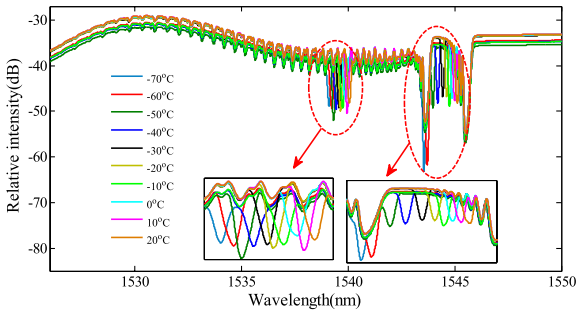

Fig. 6. (Color online) Spectra of the cascaded FBGs and TFBG at different temperatures.

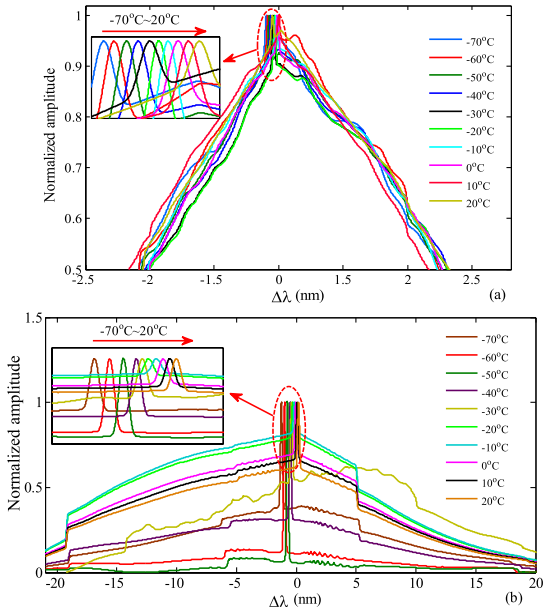

Fig. 7. (Color online) Cross-correlation curve of (a) FBG1 and (b) FBG2.

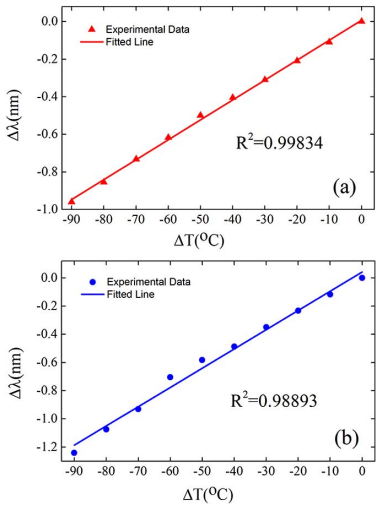

Fig. 8. Peak of the cross-correlation curve and temperature relationship of (a) FBG1 and (b) FBG2.

Table 1. Measured Errors of this Method

	Maximum error (°C)		
	Plus	Minus	Variance
FBG1	1.05	−1.30	0.72
FBG2	2.70	−3.23	2.95
TFBG	1.08	−1.46	0.89

if the wavelength range of the ASE source is from 1525 to 1565 nm, the temperature sensitivity of FBG is 13.7 pm/°C, and the measurement temperature range is from −100°C to 100°C, then in every channel of the conventional WDM the multiplexed sensors are 15 FBGs or 8 TFBGs. Using this proposed method, the multiplexed sensors are 15 FBGs and 8 TFBGs. The total number is 23, i.e., the multiplexing capability of the WDM is increased about 50%. If the power of the ASE module is 10 mW, the number of multiplexing channels can be 16, so the maximum number of sensors using this method is 368.

In conclusion, a new WDM method of FBG sensors is proposed and demonstrated based on spectrum profile identification. The wavelength of sensors can be demodulated simultaneously using a cross-correlation algorithm although they have the same central wavelengths at a channel. Using this method, the number of these multiplexed systems doubles compared to the traditional WDM system and is essential when numerous sensing points are desired.

This work was supported by the National Instrumentation Program of China (No. 2013YQ030915), the National Natural Science Foundation of China (Nos. 61227011, 61378043, 61505139, 61475114, and 11004150), the Tianjin Natural Science Foundation (No. 13JCYBJC16200), the Shenzhen Science and Technology Research Project (No. JCYJ20120831153904083), the National Basic Research Program of China (No. 2010CB327802), and the Soft Science Research and Development Project of the Ministry of Housing and Urban-Rural Development of China (No. 2016-K4-087).

References

1. Z. Y. Liu and H. Y. Tam, Chin. Opt. Lett. **14**, 120007 (2016).
2. P. Nellen, P. Mauron, A. Frank, U. Sennhauser, K. Bohnert, P. Pequignot, P. Bodor, and H. Brandle, Sens. Actuators A **103**, 364 (2003).
3. W. Wu and X. Liu, Optik **126**, 2411 (2015).
4. Y. Rao, Meas. Sci. Technol. **8**, 355 (1997).
5. S. Abad, F. Araujo, L. Ferreira, J. Santos, and M. Lopez-Amo, IEEE Sens. J. **3**, 475 (2003).
6. P. Peng, J. Lin, H. Tseng, and S. Chi, IEEE Photon. Technol. Lett. **16**, 230 (2004).
7. O. Ozolins and V. Bobrovs, Chin. Opt. Lett. **13**, 060603 (2015).
8. Y. Yu, L. Lui, H. Tam, and W. Chung, IEEE Photon. Technol. Lett. **13**, 863 (2001).
9. M. Zhang, C. Chan, D. Wang, J. Gong, W. Jin, and M. Demokan, Sens. Actuators A **100**, 175 (2002).
10. G. Lloyd, L. Everall, K. Sugden, and I. Bennion, IEEE Photon. Technol. Lett. **16**, 2323 (2004).
11. D. Cooper, T. Coroy, and P. Smith, Appl. Opt. **40**, 2643 (2001).
12. L. Ma, C. Ma, Y. Wang, D. Wang, and A. Wang, Electron. Lett. **52**, 643 (2016).
13. W. Chung, H. Tam, P. Wai, and A. Khandelwal, IEEE Photon. Technol. Lett. **17**, 2709 (2005).
14. Z. Luo, H. Wen, H. Guo, and M. Yang, Opt. Express **21**, 22799 (2013).
15. C. Caucheteur, K. Chah, F. Lhomme, M. Blondel, and P. Megret, IEEE Photon. Technol. Lett. **16**, 2320 (2004).
16. C. Huang, W. Jing, K. Liu, Y. Zhang, and G. Peng, IEEE Photon. Technol. Lett. **19**, 709 (2007).